[redacted]

211

Copy
RM L55L26a

NACA RM L55L26a

TECH LIBRARY KAFB, NM
0144166

NACA

RESEARCH MEMORANDUM

WADC
TECHNICAL LIBRARY
AFL 2811

Reg# 17374
MAR 1956

EFFECTS OF WING-BODY GEOMETRY ON THE LATERAL-FLOW ANGULARITIES AT SUBSONIC SPEEDS

By Frank S. Malvestuto, Jr., and William J. Alford, Jr.

Langley Aeronautical Laboratory
Langley Field, Va.

WADC
TECHNICAL LIBRARY
AFL 2811

[redacted]

NATIONAL ADVISORY COMMITTEE
FOR AERONAUTICS
WASHINGTON
February 21, 1956

[redacted]

[redacted]

Classification cancelled (or changed to Unclassified

By Authority of Nasa Tech Pub Announcement #123
(OFFICER AUTHORIZED TO CHANGE)

By ..... 7 Jan 58
NAME AND

..... NK
GRADE OF OFFICER MAKING CHANGE)

29 Mar 61
DATE

TECH LIBRARY KAFB, NM
0144166

NATIONAL ADVISORY COMMITTEE FOR AERONAUTICS

RESEARCH MEMORANDUM

EFFECTS OF WING-BODY GEOMETRY ON THE LATERAL-FLOW ANGULARITIES AT SUBSONIC SPEEDS

By Frank S. Malvestuto, Jr., and William J. Alford, Jr.

SUMMARY

The lateral flow characteristics in the region of a vertical tail have been investigated experimentally and theoretically at low subsonic speeds. The effects of changes in wing-body geometry such as nose position and shape, fuselage cross-sectional shape, and wing vertical position are described. The theoretical model which approximates the separated flow phenomena by a simple cylinder-vortex flow is described in an appendix.

The results indicated that a simultaneous change in nose fineness ratio and length caused an unfavorable change in the sidewash angles along the tail station. The addition of the wing to the bodies has a predominant effect on the lateral angularities, particularly at very high angles of attack. The fuselage cross-sectional shape has a marked effect on the lateral angularity produced by the wing-body combinations at low and moderate angles of attack. At high angles of attack where the effect of the wing is important, the change in lateral angularity associated with body cross-sectional shape still may be of the same order of magnitude as the sideslip angle of the airplane. The effect of raising the wing vertically on the circular cross-sectional body was to cause the sidewash angles along the tail station to become more negative.

INTRODUCTION

The estimation of the aerodynamic coefficients of an airframe, in particular the coefficients important in stability, require a knowledge of the flow fields associated with the airframe for a variety of flight conditions.

The modern airframe, characterized by a thin wing and a long body and in flight at high angles of attack, produces in many cases local fields of separated flow. These separated flows are regions of strong vortical motion or swirl and can impose irregular aerodynamic loadings on parts of the airframe that come under their influence.

The purpose of the present paper is to present some results of a low-speed experimental investigation, involving separated flow phenomena. The object of the experiment was to determine the effects of body and wing-body geometry on the lateral or sidewash angles along a line representing a possible vertical-tail station. In addition, the results of a theoretical investigation which considers the effects of separated flow are presented and are compared with experiment.

SYMBOLS

α	angle of attack, deg
β	angle of sideslip, deg
σ	angle of sidewash, deg (see fig. 1)
β_T	total angle of sidewash, deg $\left(\beta_T = \beta + \sigma;\ \text{see fig. 2}\right)$
v	sidewash velocity, positive to the right when viewed from the rear, see figure 1, ft/sec
V_∞	free-stream velocity, ft/sec
V_c	crossflow velocity in plane normal to fuselage center line, ft/sec $V_c = V_\infty \cos\beta\sqrt{\tan^2\beta + \sin^2\alpha}$
M	Mach number
z	vertical distance from fuselage surface, positive up, ft
b_v	span of vertical tail, 1.14 ft

TEST CONFIGURATIONS

Presented in figure 1 are configurations used in investigations made at a velocity of 120 miles per hour (which corresponded to a Reynolds number of 7.6×10^6 based on the original body length) in the Langley 300 MPH 7- by 10-foot tunnel, in which flow-field surveys were made by utilizing a rake of six hemispherically headed pressure probes. Each probe was instrumented to measure local pitch and sideslip angularities and dynamic pressure. The location of the survey probes for the present investigation are shown by the dashed lines labeled b_v, which are indicative of a possible vertical tail location.

Presented in figure 1 are the plan and side views of the body and wing. The wing had 45° sweepback of the quarter-chord line, an aspect ratio of 4, a taper ratio of 0.3, and NACA 65A006 airfoil sections parallel to the fuselage center line. Also shown in figure 1 are the three different fuselage cross-sectional shapes investigated. These shapes included a circular cross section, a rectangular cross section with major length horizontal, and a rectangular cross section with the major length vertical. For the two rectangular cross sections, the major length was 50 percent greater than the minor length and all corners were rounded. For all three fuselages the axial distribution of cross-sectional area was identical.

For the fuselage of circular cross section, tests were also made to determine the effects of changes in nose length and nose shape. The original ogival nose was moved forward by 50 percent of its length by the insertion of a cylindrical section at its base. The second nose modification was to replace the original nose plus the cylindrical insert with an elongated ogive.

RESULTS AND DISCUSSION

Effect of Isolated Body Geometry

The effects of isolated body geometry, for the circular cross section, on the sidewash angularity along a vertical line representative of a possible vertical-tail location are presented in figure 2 for an angle of attack of 24° and a sideslip angle of 5°. Shown on the right are the calculated total angularity contours in a crossflow plane, that is, in a plane that cuts the body normal to its longitudinal axis.

The symbol V_c represents the component of the free-stream velocity in this plane, that is, the crossflow velocity. This velocity makes an angle with the vertical because the body is at an angle of sideslip. The contours are for the case where the flow has separated and can be approximately represented by a vortex pair symmetrically placed with respect to the direction of the crossflow velocity.

The locations and strengths of the vortices were estimated by a simple theoretical procedure that is described in the appendix. This procedure allows the estimation of the vortex paths and strengths from the nose to the rear of the body and is dependent upon a knowledge of the viscous force acting on the nose or expanding section of the body and of the viscous-force distribution along the cylindrical afterbody.

The effect of flow separation approximated in terms of the vortex pair is seen to be important. For example, along the dashed vertical

line above the body where a vertical tail is generally located, the angularity is positive and increases in magnitude as the vortices are approached. It should be noted that these positive angularities are in a direction to decrease the angle of sideslip β of the airplane and are therefore generally considered favorable from stability considerations. Below the vortex pair the angles are seen to be negative and quite large in magnitude. In contrast to the positive angles, these negative angles tend to increase the angle of sideslip and are therefore considered unfavorable.

In order to show more clearly the magnitudes and directions of the sidewash angularities a cross plot of the theoretical values along the vertical line are presented on the left part of figure 2, along with the experimentally determined angles. The change in the sign of the lateral angularities mentioned earlier is now evident. The qualitative agreement between the experiment and predicted angularities implies that the separated flow is indeed vortical and that the assumed vortex model is useful in qualitative studies of the lateral flow.

Effect of Nose Length and Nose Shape

The effects of nose length and nose shape on the induced sidewash angle σ for the body of circular cross section are presented in figure 3. The conditions depicted are for an angle of attack of 16° and an angle of sideslip of 5°.

Consider first the effect of change in nose location. The nose was moved forward by 50 percent of its length by the insertion of a cylindrical segment at its base. The corresponding angularity variations with vertical distance are seen to show little effect of moving the original nose forward (fig. 3). The original nose plus the inserted cylindrical section were then replaced by a new nose of ogival shape and having the same length as the original nose plus the cylindrical section. This change in nose geometry has a noticeable effect on the induced sidewash angularity variation and moves the crossover point from positive to negative sidewash to a higher location relative to the crossover point for the original configuration and for the forward-nose configuration.

Preliminary theoretical studies indicate that the larger viscous force associated with this last mentioned modification of the nose section results in stronger vortices located higher in the nose-base plane relative to the other arrangements and hence results in the vortex pair remaining higher above the afterbody as they travel downstream, whereby the crossover point from positive to negative angles was higher, as shown in figure 3.

Effect of Body Cross-Sectional Shape

The effects of body cross-sectional shape on the induced sidewash angles along the vertical tail station for a moderate attitude ($\alpha = 8^{\circ}$, $\beta = 5^{\circ}$) are presented in figure 4. Shown on the left are the wing-off results and on the right are results with a 45° swept wing attached to the bodies to provide a midwing configuration. The wing-off results (fig. 4) indicate that for all cross sections, both circular and rectangular, the variation of the angularity with vertical distance is generally the same and the crossover from positive to negative angularities occurs at approximately the same vertical distance above the body. It should be noted, however, that the rectangular cross section with major length vertical gives results that are somewhat more favorable than the others.

From examination of the angularity variations for the midwing-body combination (fig. 4), the effect of wing-body interference for the different body cross sections is evident, especially on the lateral flow along the part of the tail near the body, where the tail loading is generally predominant. It is observed that the effect of this interference is to cause the induced angularity above the circular fuselage to become unfavorable (more negative) and to cause the induced angularity above the rectangular shapes to become more favorable (more positive.) Similar effects of wing-body interference for the different cross-section shapes have also been observed at an angle of attack of 16° and an angle of sideslip of 5°.

In order to give some indication of the angularity variation along the vertical-tail station at a rather high attitude, the results for both the wing-off and the midwing configurations at an angle of attack of 24° and an angle of sideslip of 5° are presented in figure 5. It is to be noted that for this high-attitude condition the body-alone results show a marked effect of body cross section on the flow separations and hence on the flow-angularity variations. Examination of the wing-body results for this high attitude (fig. 5) indicates that the wing vortex streams predominate. This result might be explained by noting that the wing downwash field accompanying the strong vortex flow of the wing will tend to deflect the body vortices and thereby minimize the effect of body vortex flow and, hence, of cross section on the lateral angularity along the vertical tail station. Unpublished wing-alone results follow very closely the angularity variations shown for the wing-body combinations and support the statements that for this high attitude the wing-flow effects are predominant.

A word of caution is necessary regarding the order of differences between the angularity characteristics for the different wing-body combinations, which appear small when compared with the corresponding wing-off angularity characteristics. It should be noted that these apparently small differences for the wing-body combination are, in some

cases, of the order of 5°, which is the angle of sideslip of the configuration. These differences therefore can contribute to significant changes in the force and moment contribution of a vertical tail immersed in the flows of the different wing-body combinations.

Effect of Wing Height

The effect of vertical position of the wing on the sidewash angularities along the vertical tail station are presented in figure 6 for the circular-cross-section wing-body combinations. Shown on the left of the figure are the characteristics for the moderate attitude of $\alpha = 8^{\circ}$, $\beta = 5^{\circ}$ and on the right, the characteristics for the high attitude of $\alpha = 24^{\circ}$, $\beta = 5^{\circ}$. Presented for comparison are the body-alone characteristics for the same attitudes.

At the moderate attitude the high-wing position is seen to be the least favorable. The wing in this position tends to deflect somewhat the body vortices. At the high attitude the predominant effect of the wing is again evident. It should be observed that the higher the wing is placed on the body, the higher are the wing vortices relative to the vertical-tail station; and hence the crossover from positive to negative angularity occurs at a higher location along the vertical-tail station. This higher location of the crossover point results in a greater portion of the angularity distribution being negative along the tail station and, therefore, an increased unfavorable effect on stability. It should also be noted that, at the high attitude, the effect of wing vertical position (fig. 6) is stronger than the effect of body cross-sectional shape (fig. 5).

CONCLUDING REMARKS

An experimental and theoretical investigation of the lateral flow characteristics in the region of a vertical tail has been discussed. The following results are indicated:

1. The concept of a simple vortex model is useful in the qualitative analysis of the separated-flow phenomena associated with an isolated pointed nose body of revolution at an angle of attack.

2. The effect of increasing the length and fineness ratio of the body nose is to cause an unfavorable contribution to the lateral angularities along the vertical-tail station.

3. The addition of a wing to the body has a predominant effect on the lateral angularities but the effect of fuselage cross-sectional shape produces changes in the sidewash angles that may be of the same order of magnitude as the sideslip angle of the airplane.

4. The effect of raising the wing vertically, on the circular-cross-section body, is to cause the sidewash angles along the vertical tail to become more unfavorable.

Langley Aeronautical Laboratory,
National Advisory Committee for Aeronautics,
Langley Field, Va., November 2, 1955.

APPENDIX

ESTIMATION OF VORTEX STRENGTH AND POSITION IN BASE PLANE OF EXPANDING NOSE SECTION

The object of this appendix is to discuss briefly an approximate method now under way at the Langley Laboratory for estimating the position and strength of a vortex pair that is assumed to represent the vortex wake pattern that exists on the lee side of a slender, pointed nose, lifting body of revolution. The wake pattern is by no means as simple, as is evident from visual studies of the flow made by water-tank and vapor-screen techniques (refs. 1 to 4). For slender, pointed-nose bodies, however, the development of the flow over the expanding nose section seems to consist of two well-defined spiral surfaces of separation that grow continuously as the expanding nose section is traversed from the front to the rear. The predominant effect of this type of separation seems to occur in planes normal to the longitudinal axis of the body, that is, in the so-called crossflow planes.

In a crossflow plane, fixed in space, that is traversed by the body, the type of flow separation under discussion appears similar to the separated flow about a two-dimensional circular contour that is impulsively set in motion. This association between the body crossflow and the two-dimensional cylinder flow was pointed out and discussed in references 1 and 2.

For the present purpose it is tacitly assumed that the flow separation behind a slowly expanding two-dimensional cylinder moving in a downward direction is a good approximation to the flow separation in the fixed crossflow plane traversed by the body. The implication here of course is that along the body the separation surfaces grow conically in the axial direction. In addition, the assumption is made that the spiral separation surfaces of vorticity can be approximated by a potential vortex pair that are symmetrically located with respect to the direction of the component of the resultant free-stream velocity in the crossflow plane. (See fig. 2.) With these assumptions in mind, it is clear that the simplified analytical model that will be used to approximate the actual flow is that of a two-dimensional, cylinder-vortex flow in which the cylinder expands and the flow changes homogeneously with time. It is to be emphasized that the use of a cylinder-vortex-flow model has been considered by other authors to depict the flow over lifting slender bodies. (See refs. 4 to 7.)

Consider now the local aerodynamic force acting on the cylindrical trace of the body in the fixed crossflow plane as the body passes through this plane. With respect to a system of axes fixed to the downward moving two-dimensional cylinder in this plane, the local vertical force dN for zero sideslip may be expressed as follows:

$$dN = dN_o + \left[\frac{D}{Dt}I + \rho\frac{D}{Dt}\Sigma z_i\Gamma_i\right]dx \tag{1}$$

where

N_o slender-body potential-flow force derived by Munk

$-I$ momentum of fluid induced by vortices in the presence of the body

z_i location of each vortex relative to the fluid

D/Dt total differential operator

t time, sec

Γ_i circulation of each vortex (Γ is absolute value)

x axial coordinate of body

The term $\frac{D}{Dt}I$ can be considered as the negative of the total rate of change of the fluid momentum induced by the vortices in the presence of the body (ref. 8). The last term may be considered as the concentrated force that would be required to move the vortices with a given velocity for unsteady motion (ref. 8).

For the cylinder-vortex flow under consideration, the quantity I is given by

$$I = -2\rho_\infty\frac{a^2}{r}\sin\gamma\,\Gamma + 2\rho_\infty r\sin\gamma\,\Gamma \tag{2}$$

where

a local radius of body in crossflow plane

r distance from center of body to vortex element

γ acute angle between r and crossflow direction

Now if, as stated previously, it is assumed that the flow separation is conical, the vortex pair remains stationary with respect to the expanding contour of the moving cylinder in the fixed crossflow plane and hence the concentrated force term of equation (1) is equal to zero.

There remain to be determined the relations between the vortex strength Γ and the position (r, γ) of the vortices. In the fixed crossflow plane the equilibrium position of the vortex pair can be obtained from the Foppl relations which relate the locus of positions of the symmetrical vortex pair to the strength of the vortices required for the vortex pair to remain stationary. The Foppl relations may be expressed as

$$2r \sin \gamma = r - \frac{a^2}{r} \tag{3}$$

which is the equation of the curve that the vortices must lie on for equilibrium. The relation

$$\begin{aligned} \Gamma &= 2\pi V_c r\left(1 - \frac{a^2}{r^2}\right)^2\left(1 + \frac{a^2}{r^2}\right) \\ &= 2\pi V_c r H(\lambda) \end{aligned} \tag{4}$$

gives the strength of the vortices in terms of their position and the crossflow velocity V_c. Note that Γ has the required conical variation with r.

The substituion of the necessary preceding relations into expression (1) for the local force and replacement of dN_o by $2\rho\pi V_\infty^2 \cos \alpha \sin \alpha\, a\left(\frac{da}{dx}\right)dx$ yields (with $x = tV_\infty \cos \alpha$ as the axial coordinate):

$$\begin{aligned} dN = {} & 2\rho\pi V_\infty^2 \cos \alpha \sin \alpha\, a\, da + \\ & 4\rho\pi V_\infty^2 \cos \alpha \sin \alpha\left(\frac{1}{\lambda} - 1\right)(1 - \lambda^2)H(\lambda)a\, da \end{aligned} \tag{5}$$

By use of the relation $C_N = \frac{N}{\frac{1}{2}\rho V_\infty^2 \pi a_b^2}$, equation (5) can be nondimensionalized and yields, after integration from $a = 0$ to $a = a_b$ (the radius of the base of the nose section):

$$C_N = 2 \cos \alpha \sin \alpha + 4\left(\frac{1}{\lambda} - 1\right)\left(1 - \lambda^2\right)H(\lambda)\cos \alpha \sin \alpha \tag{6}$$

Equation (6) gives the total force acting on the nose section in terms of the position of the vortex pair, since γ, the angular coordinate of the position, is according to relation (3) a function of $\lambda = \frac{a}{r}$. From equation (6), it is then possible to determine the position of the vortex pair provided a knowledge of C_N or of $\left(C_N - 2 \cos \alpha \sin \alpha\right)$, the viscous force, is available. (See refs. 3 and 9.) Once r and γ are known the vortex strength Γ can be determined from equation (4) and the lateral velocities and angularities can then, of course, be calculated by classical methods.

If the body has a cylindrical aftersection, the strength and position of the vortices determined in the base of the expanding section will serve as initial conditions for estimating the vortex path along the afterbody, using the procedures set forth by Jorgensen and Perkins in reference 4. This method requires a knowledge of the viscous force distribution along the afterbody sections.

The reader should be cautioned that the preceding first-order results for the estimation of vortex position and strength are tentative. Detailed examination of the assumptions and approximations are needed, particularly in regard to the effect of (a) the replacement of the surfaces of separation by a symmetrical vortex pair which introduces a multivaluedness in the pressure field that is not correct and (b) the stability of the vortex pair for conical type flows.

It should also be noted that the preceding analysis is for zero sideslip. The derived relations are, of course, valid for the sideslip condition provided that the crossflow velocity V_c for sideslip is used and the vortices located symmetrically with respect to this sideslip crossflow velocity direction. The force C_N is the force parallel to this direction.

REFERENCES

1. Allen, H. Julian: Pressure Distribution and Some Effects of Viscosity on Slender Inclined Bodies of Revolution. NACA TN 2044, 1950.

2. Gowen, Forrest E., and Perkins, Edward W.: A Study of the Effects of Body Shape on the Vortex Wakes of Inclined Bodies at a Mach Number of 2. NACA RM A53I17, 1953.

3. Allen, H. Julian, and Perkins, Edward W.: Characteristics of Flow Over Inclined Bodies of Revolution. NACA RM A50L07, 1951.

4. Jorgensen, Leland H., and Perkins, Edward W.: Investigation of Some Wake Vortex Characteristics of an Inclined Ogive-Cylinder Body at Mach Number 1.98. NACA RM A55E31, 1955.

5. Michelson, I.: On the Motion of Vortices Behind a Circular Cylinder. TM-377 (Task Assignments NOTS-Re3d-441-3), U.S. Naval Ordinance Test Station, Oct. 29, 1951.

6. Lagerstrom, P. A., and Graham, M. E.: Aerodynamic Interference in Supersonic Missiles. Rep. No. SM-13743, Douglas Aircraft Co., Inc., July 1950.

7. Kuchemann, D.: A Non-linear Lifting-Surface Theory for Wings of Small Aspect Ratio with Edge Separations. Rep. No. Aero. 2540, British R.A.E., Apr. 1955.

8. Sedov, L. I.: On the Theory of the Unsteady Motion of an Airfoil. NACA TM 1156, 1947.

9. Kelly, Howard R.: The Estimation of Normal-Force, Drag, and Pitching-Moment Coefficients for Blunt-Based Bodies of Revolution at Large Angles of Attack. Jour. Aero. Sci., vol. 21, no. 8, Aug. 1954, pp. 549-555, 565.

SKETCH OF WIND-TUNNEL MODEL USED FOR SIDEWASH-ANGULARITY MEASUREMENTS

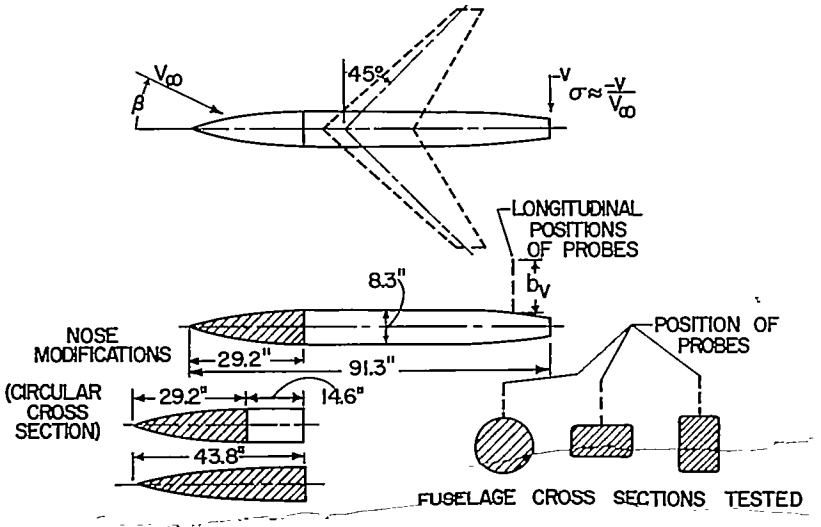

Figure 1

ILLUSTRATION OF CALCULATED TOTAL SIDEWASH ANGULARITIES IN BODY CROSS-FLOW PLANE

CIRCULAR CROSS-SECTION; α=24°, β=5°

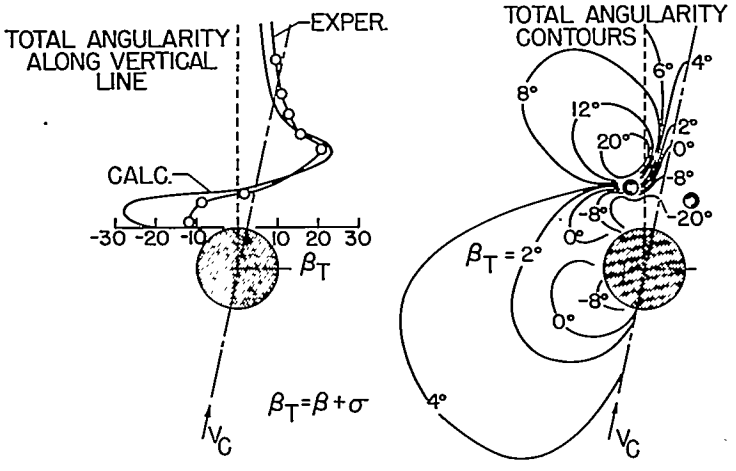

Figure 2

EFFECT OF BODY NOSE CHANGES ON SIDEWASH ANGULARITY
BODY OF CIRCULAR CROSS-SECTION

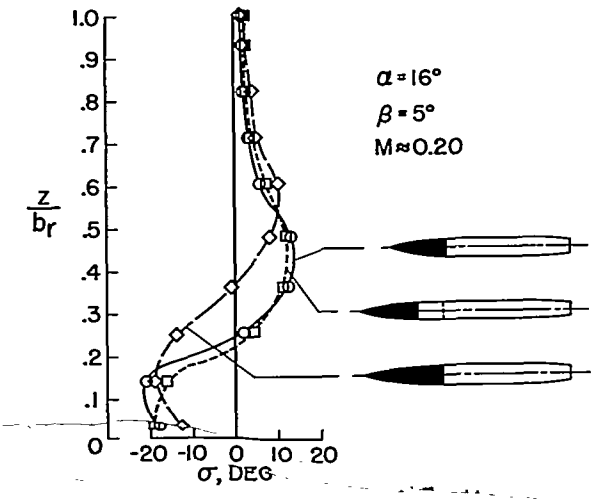

Figure 3

THE EFFECT OF BODY CROSS SECTION ON SIDEWASH ANGULARITY
M ≈ 0.20

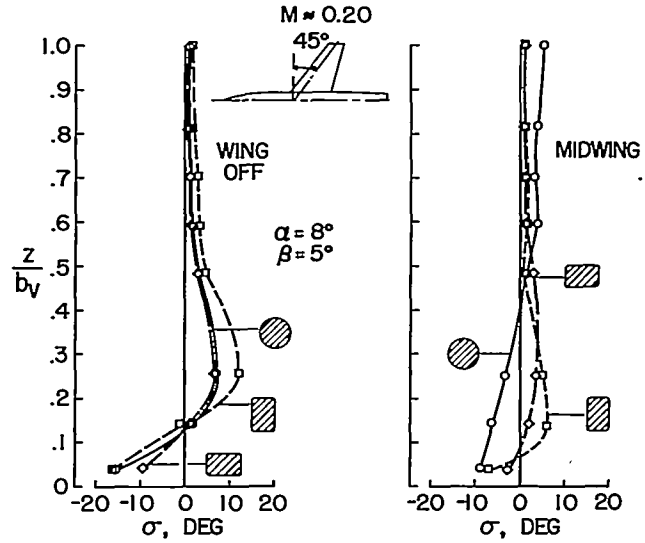

Figure 4

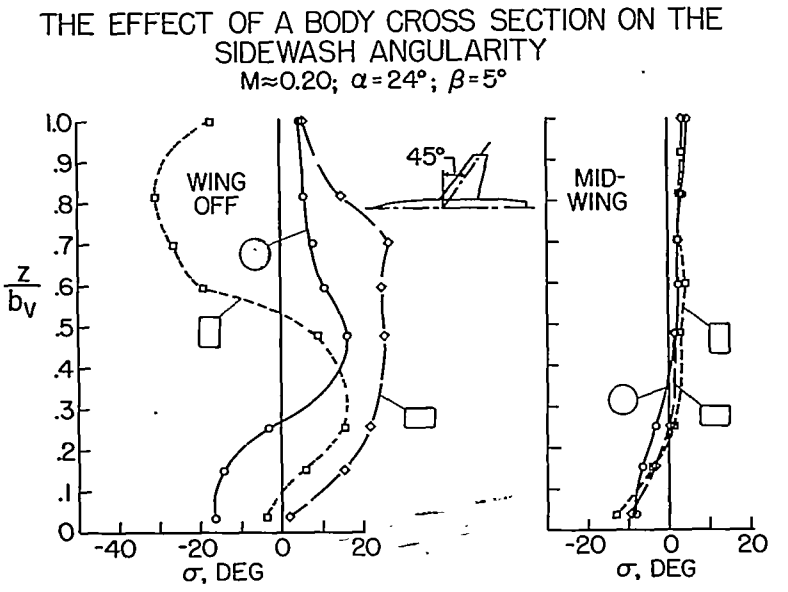

Figure 5

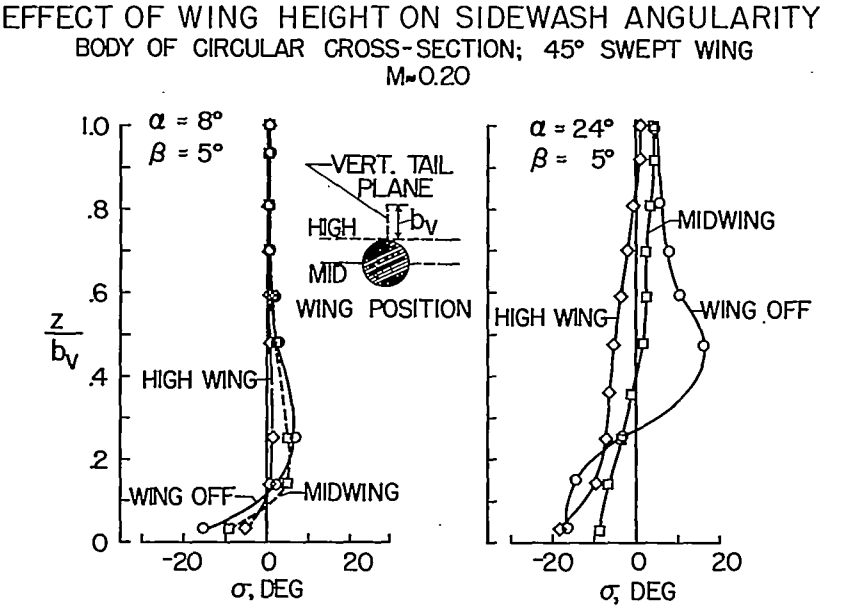

Figure 6